SUPPLEMENTARY MATERIAL

"Associated patterns of insecticide resistance in field populations of malaria vectors across Africa"

Penelope A. Hancock[a1], Antoinette Wiebe[a], Katherine A. Gleave[b], Samir Bhatt[c], Ewan Cameron[a], Anna Trett[b], David Weetman[b], David L. Smith[d], Janet Hemingway[b], Michael Coleman[b], Peter W. Gething[a], Catherine L. Moyes[a1]

S1. Bioassay data: selection criteria and spatio-temporal distribution.....1
S2. Posterior validation for models incorporating pyrethoids and DDT.....6
S3. Predicted cross-insecticide interaction strengths for models incorporating pyrethroids and DDT.....13
S4. Predicted resistance relationships across the other insecticide combinations.....14
S5. Analysis of linear associations between DDT and pyrethroid resistance and the prevalence of *Vgsc* point mutations.....15
S6. Spatio-temporal Bayesian statistical models.....16
S7. *Vgsc* allele frequency data selection criteria.....18

S1. Bioassay data: selection criteria and spatio-temporal distribution

Our insecticide resistance bioassay data set includes information about the mosquitoes tested, the number of mosquitoes in the sample, the sample collection and the bioassay conditions and protocol (1). Some of this information was used to select a subset of records for inclusion in our study, including the mosquito sample identification data (available at either the genus, complex or species level), the collection site location, the bioassay protocol, the insecticide tested and whether a synergist was used, and the insecticide concentration and exposure period (1). We only included bioassays that were conducted over the period 2000-2015 on samples collected within two separate spatial regions: a rectangular region in West Africa that extends from 0°N to 16.3°N and -18°W to 19°W, and a rectangular region in East Africa that extends from -28°N to 16.5°N and 24.5°W to 51.5°W (Fig. 1). Only bioassay results for which the sample collection location was assigned a point coordinate were included, noting that for these bioassays the collection area is less than 25km^2 (1). Further, we consider only bioassays conducted on mosquito samples that were identified as belonging to the *An. gambiae* complex. The majority of these studies (~80%) did not identify the individual species within the *An. gambiae* complex to which the sampled mosquitoes belonged, therefore our study does not account for differences in insecticide resistance phenotypes that can occur across these sibling species (2-11).

We included bioassays conducted using insecticides from four different classes (Fig. 1). For pyrethroids this included three insecticides: deltamethrin, permethrin and λ-cyhalothrin. For organochlorines, only bioassays conducted using DDT were included, and for carbamates only bioassays conducted using bendiocarb were included. For organophosphates, our data subset for the west Africa region includes only bioassays that used fenitrothion, while for the east Africa region our data includes bioassays that used both fenitrothion and

malathion. Bioassays for which the insecticide concentration or the exposure time differ from that defined by the standard WHO insecticide susceptibility bioassay protocol (12) were excluded from the analysis. Also excluded were any bioassays performed on a sample of less than 20 mosquitoes and any bioassays that used synergists.

The final data set included a total of 5,595 data points that met these criteria (see Table S1 for a breakdown by insecticide type and across the east and west regions). We note that this dataset does not provide mortality values for all of the insecticides of interest at each of the 1,183 locations so associations among these insecticides cannot be analysed directly. For example, for pyrethroids, there are only 20 point locations for which we have 5 or more records for two different pyrethroid types. Further the spatiotemporal distribution of data for each insecticide is not uniform or random and each distribution incorporates sampling biases (Fig. 1 and Figs. S1-S4). For these reasons we evaluated the relationships among the insecticides by incorporating these datasets from field populations into a geostatistical model.

	No. bioassay results		**No. unique locations**	
Insecticide	**East**	**West**	**East**	**West**
Pyrethroids				
deltamethrin	732	747	405	485
permethrin	522	504	321	317
λ-cylohalothrin	364	194	246	132
Organochlorines				
DDT	552	597	370	403
Organophosphates				
fenitrothion	148	268	100	150
malathion	141	-	119	-
Carbamates				
Bendiocarb	385	441	256	248
Total	**5,595**		**1,183**	

Table S1. Number of bioassay data points available for each insecticide in each region.

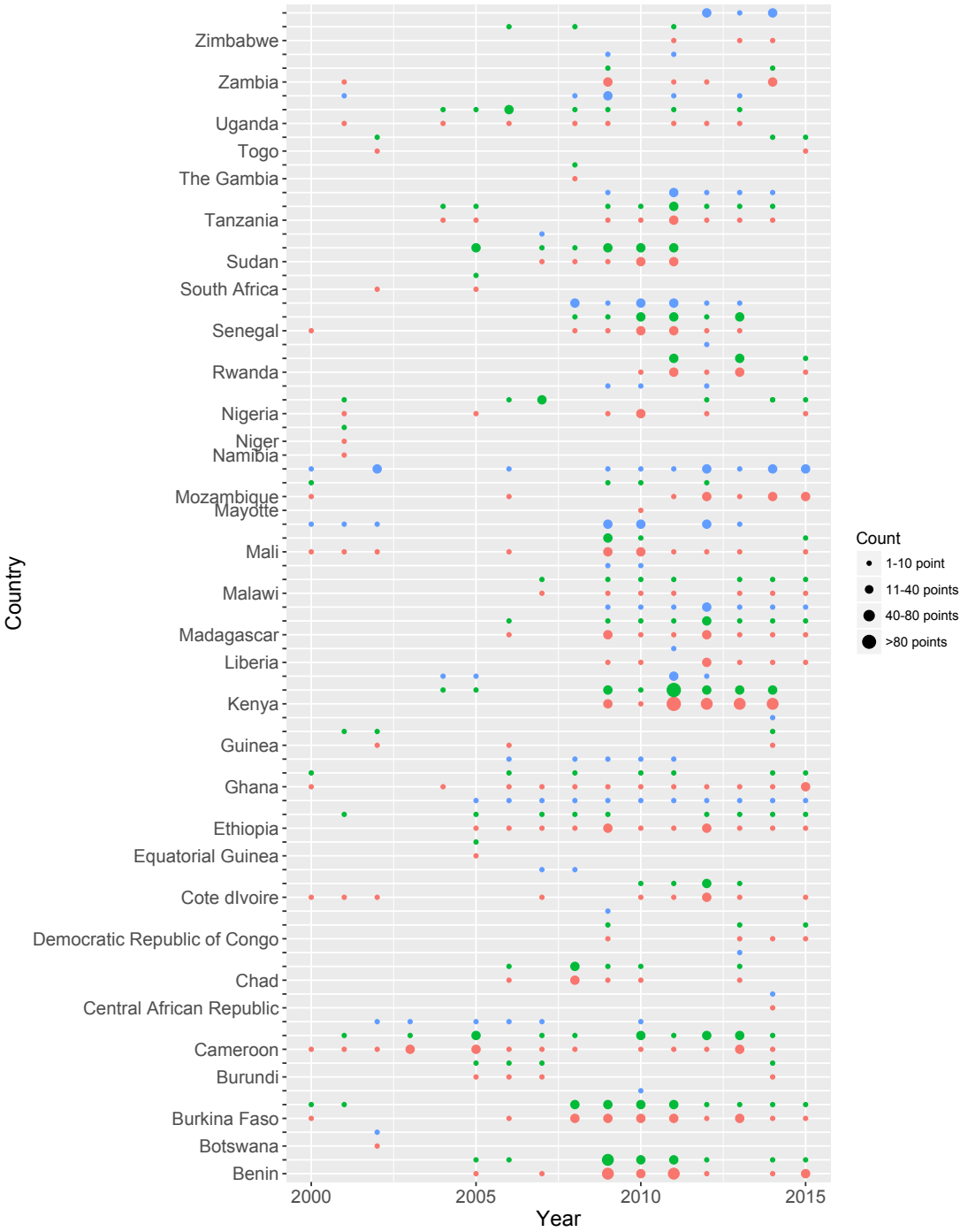

Figure S1. The number of bioassay records for the three pyrethroid types, deltamethrin (red), permethrin (green) and λ-cyhalothrin (blue) by country and year.

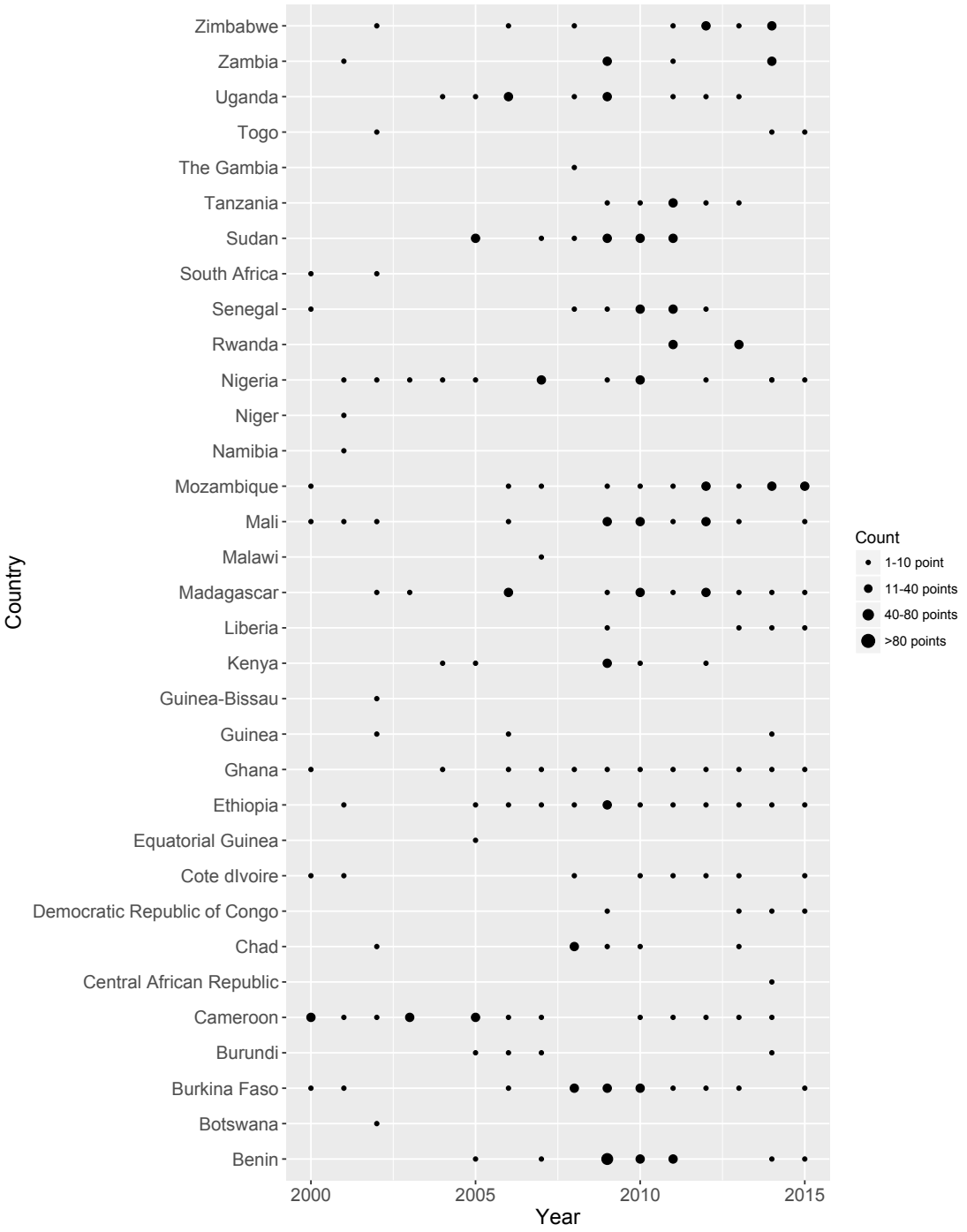

Figure S2. The number of DDT bioassay records by country and year.

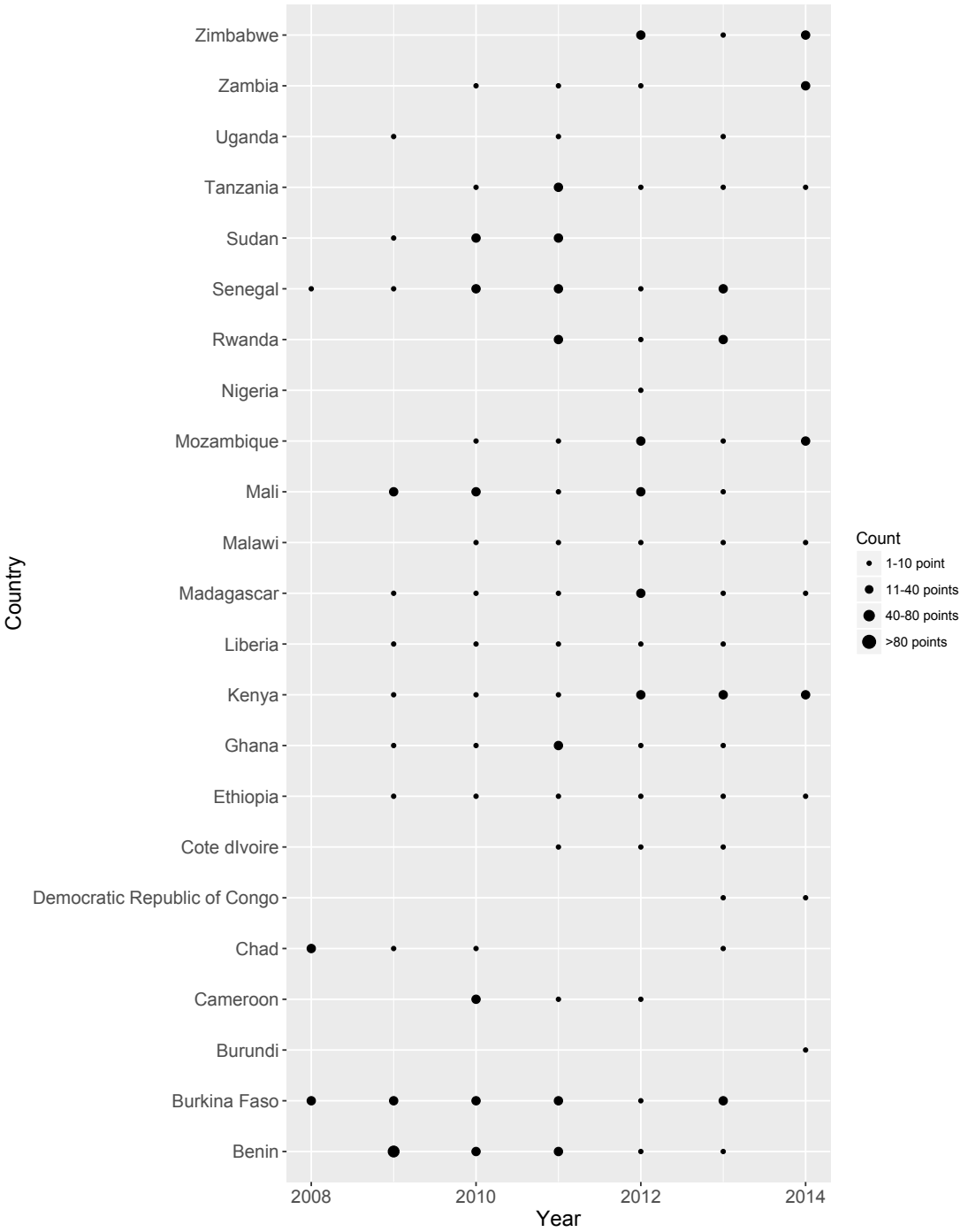

Figure S3. The number of bendiocarb bioassay records by country and year.

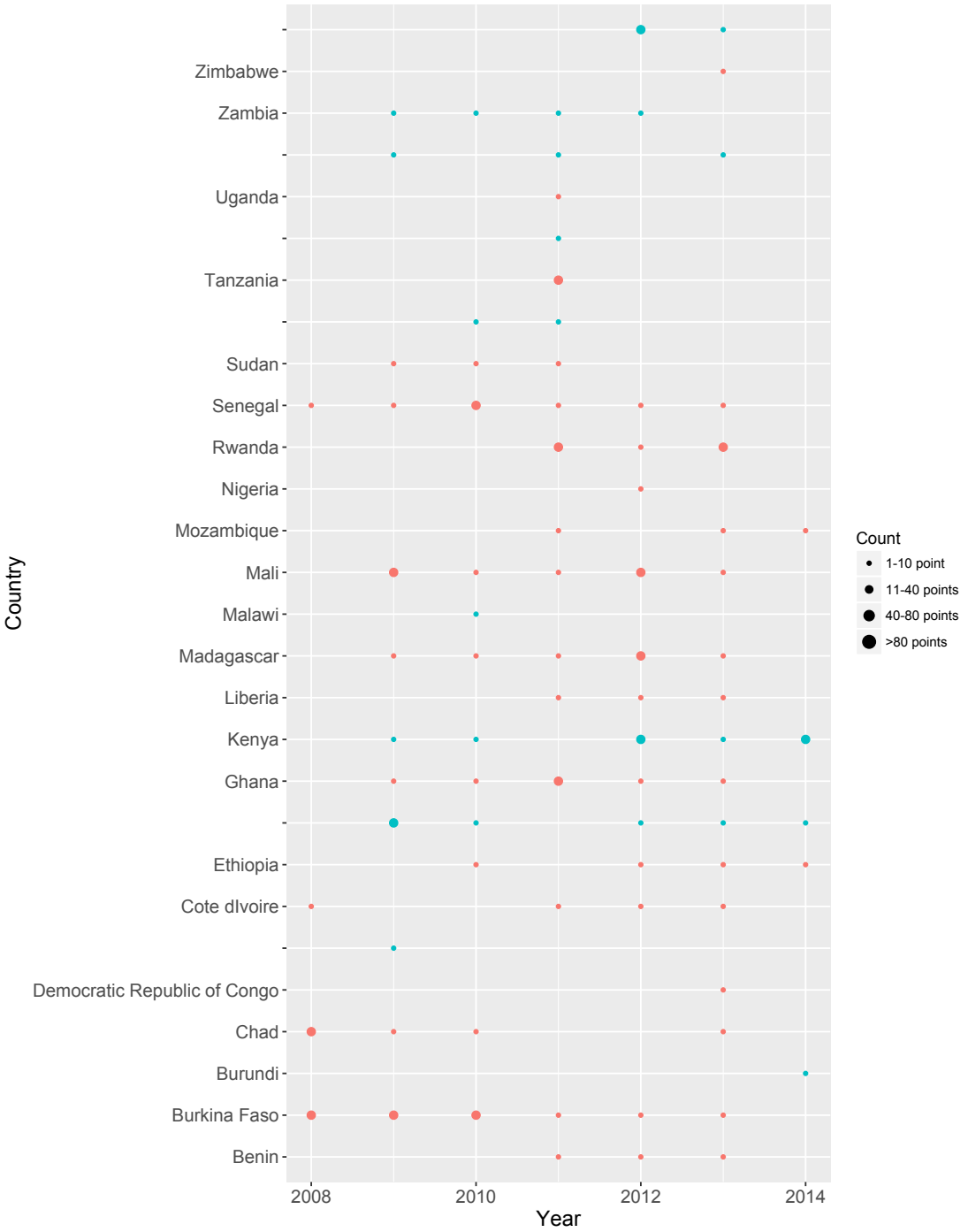

Figure S4. The number of bioassay records for the two organophosphates, fenitrothion (red) and malathion (blue) by country and year.

S2. Posterior validation for models incorporating pyrethoids and DDT

We present posterior validation results for the linear models of coregionalization (LMCs) that were preferred over models that assumed resistance phenotypes did not interact across insecticides. These models are described in the main text, and include LMCs that jointly modelled resistance to the three pyrethroid types (deltamethrin, permethrin and λ-cyhalothrin) as well as LMCs that jointly modelled resistance between these three pyrethroids and DDT. For these models we verified that the probability integral transform (PIT) histograms were approximately uniform (Figs. S5 & S6). For each insecticide type $I \in \{A, B, C, D\}$,

10-fold out-of-sample cross validation was performed by fitting the models to ten subsets of the proportional mortality data where each data subset was created by withholding a randomly selected sample of v_I data points, where v_I was set to 10% of the total number of records for insecticide type I. We use these out-of-sample predictions to verify the predictive accuracy of our models (Figs. S7-S9). We also use the root mean squared error (RMSE) of the out-of-sample predictions to support the comparison of WAIC values across the two model types described above. Finally, we verified that the distribution of the observed proportional mortality values across all space-time locations was similar to that of co-located simulations from the posterior, based on 1000 simulated data sets (Fig. S11 & S12).

S2.1. Probability integral transform histograms

The probability integral transform (PIT) is calculated from the value of the cumulative predictive distribution at the observation locations and times (13). If the observations follow the predictive distribution, the distribution of the PIT values across the observation locations and times is approximately uniform. The R-INLA package (http://www.r-inla.org) provides approximate cross-validated PIT values where the PIT value for observation i is adjusted to omit the contribution of the i^{th} observation to the posterior predictive distribution (14). We use PIT histograms to assess the calibration of out-of-sample predictions. The PIT histograms are approximately uniform for the LMC model for pyrethroids (Fig. S5) and the LMC model for DDT and pyrethroids (Fig. S6).

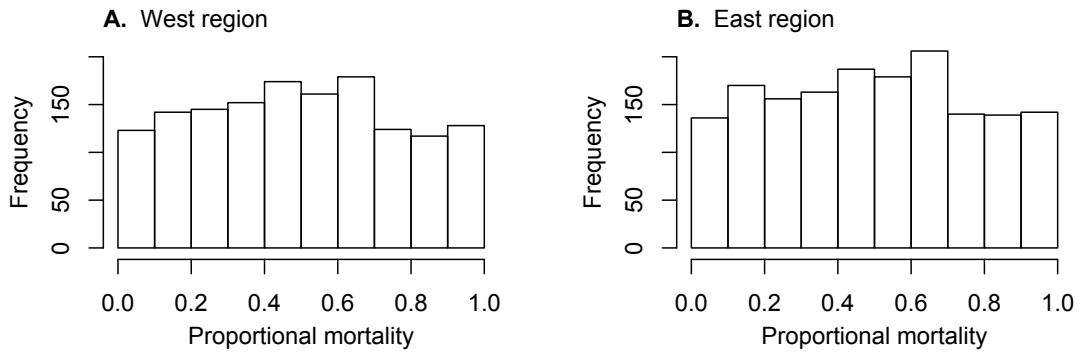

Figure S5. Histograms of the PIT values comparing observations and cumulative predictive densities for the LMC that includes bioassay observations for the three pyrethroid types, deltamethrin, permethrin and λ-cyhalothrin.

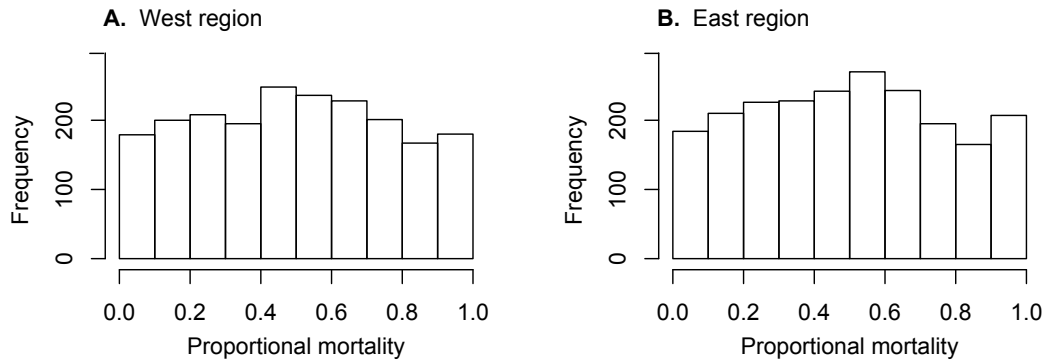

Figure S6. Histograms of the PIT values comparing observations and cumulative predictive densities for the LMC that includes bioassay observations for DDT and the three pyrethroid types, deltamethrin, permethrin and λ-cyhalothrin.

S2.2. K-fold out-of-sample validation

For each insecticide type, 10-fold out-of-sample cross validation was performed by fitting the models to ten subsets of the proportional mortality data where each data subset was created by withholding a randomly selected sample of v_I data points, where v_I was set to 10% of the total number of records for insecticide type I (Table S2). The LMC for pyrethroids produced a lower out-of-sample RMSE than the model which excluded interactions between resistance across insecticides for all insecticides, except for permethrin for the west region, where the RMSE for the two models was the same (Table S2). The LMC for DDT and pyrethroids produced a lower RMSE for DDT resistance predictions for the west region but the RMSE for the east region was the same for the two models (Table S2). For models incorporating other combinations of insecticides the RMSE was the same or higher than that produced by the model which excluded interactions (Table S2).

Plots of the out-of-sample predicted means against the observed values for the LMC model for pyrethroids for the west region (Fig. S7) and the east region (Fig. S8) show that the majority of predictions are accurate but some observations have large deviations from the predicted mean. A similar pattern arises in comparing the observed DDT resistances to the predicted means (Fig. S9). We attribute these deviations to the high sampling variability of the bioassay observations and the sparse spatio-temporal coverage of the data (Fig. 1 and Figs. S1-S4).

Insecticide bioassays included in model	**Out-of-sample RMSE**			
	West region		**East region**	
	LMC	**No interactions**	**LMC**	**No interactions**
D,P,L	0.20 (D) 0.21 (P) 0.18 (L)	0.21 (D) 0.21 (P) 0.20 (L)	0.15 (D) 0.17 (P) 0.16 (L)	0.16 (D) 0.20 (P) 0.17 (L)
Och,D,P,L	0.19 (O)	0.20 (O)	0.18 (O)	0.18 (O)
Ca,D,P,L	0.15 (B)	0.15 (B)	0.15 (B)	0.13 (B)
Oph,D,P,L	0.1 (Oph)	0.1 (Oph)	0.1 (Oph)	0.09 (Oph)
Och,Ca	0.17 (O) 0.15 (B)	0.17 (O) 0.15 (B)	0.19 (O) 0.15 (B)	0.19 (O) 0.12 (B)

Och, Oph	0.17 (O) 0.09 (Oph)	0.17 (O) 0.09 (Oph)	0.22 (O) 0.08 (Oph)	0.19 (O) 0.08 (Oph)
Ca, Oph	0.15 (B) 0.09 (Oph)	0.15 (B) 0.09 (Oph)	0.15 (B) 0.08 (Oph)	0.12 (B) 0.08 (Oph)

Table S2. The out-of-sample RMSE for predicted resistance to each insecticide for an LMC and a model where resistances do not interact across different insecticides. Independent models are fitted to the west and east regions. The insecticide bioassays included in the two models are denoted as follows: deltamethrin (D), permethrin (P), λ-cyhalothrin (L), DDT (Och), bendiocarb (Ca), organophosphates including fenitrothion for the west region and both fenitrothion and malathion for the east region (Oph). For models that consider resistances to all pyrethroids together with resistances to an insecticide from another class, resistances to the three pyrethroids are modelled using an LMC that allows interactions between resistances across the pyrethroid types (see text).

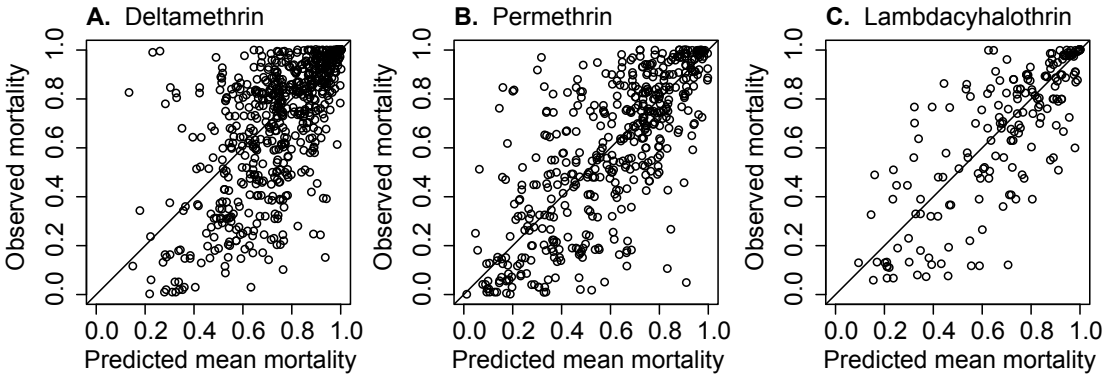

Figure S7. Comparing withheld bioassay mortality observations with the mean mortality predicted by the LMC for pyrethroids for the west region.

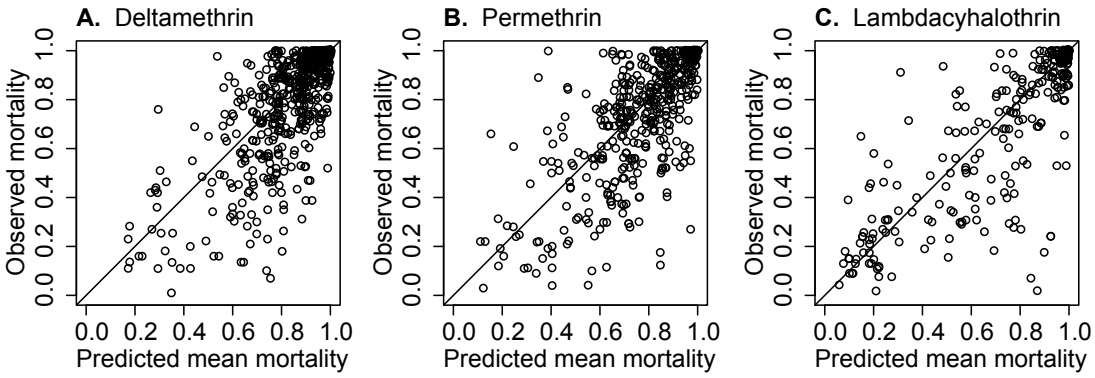

Figure S8. Comparing withheld bioassay mortality observations with the mean mortality predicted by the LMC for pyrethroids for the east region.

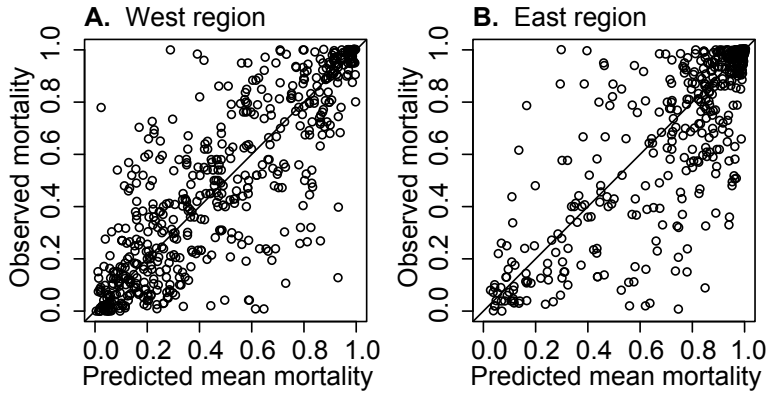

Figure S9. Comparing withheld DDT bioassay mortality observations with the mean mortality predicted by the LMC for DDT and pyrethroids.

S2.3. Comparison of pointwise WAIC values

In addition to our comparison of the WAIC given by the LMC model and a model which excluded interactions between resistance across insecticides, we compared the distributions of the contribution of each data point to the WAIC produced by the two models. In the case of the models for predicting resistance to the three pyrethroids, a greater proportion of the data have lower WAIC values for the LMC (Fig. S10A & B), although for both models there are some observations that are less accurately predicted and have much higher WAIC values. For the models used to predict resistance to both DDT and the three pyrethroids, the LMC also produced a greater proportion of smaller WAIC values than a model that excluded interactions across the two insecticide classes (Fig. S10C & D), but the difference between the two models is less than that produced by excluding interactions among pyrethroids.

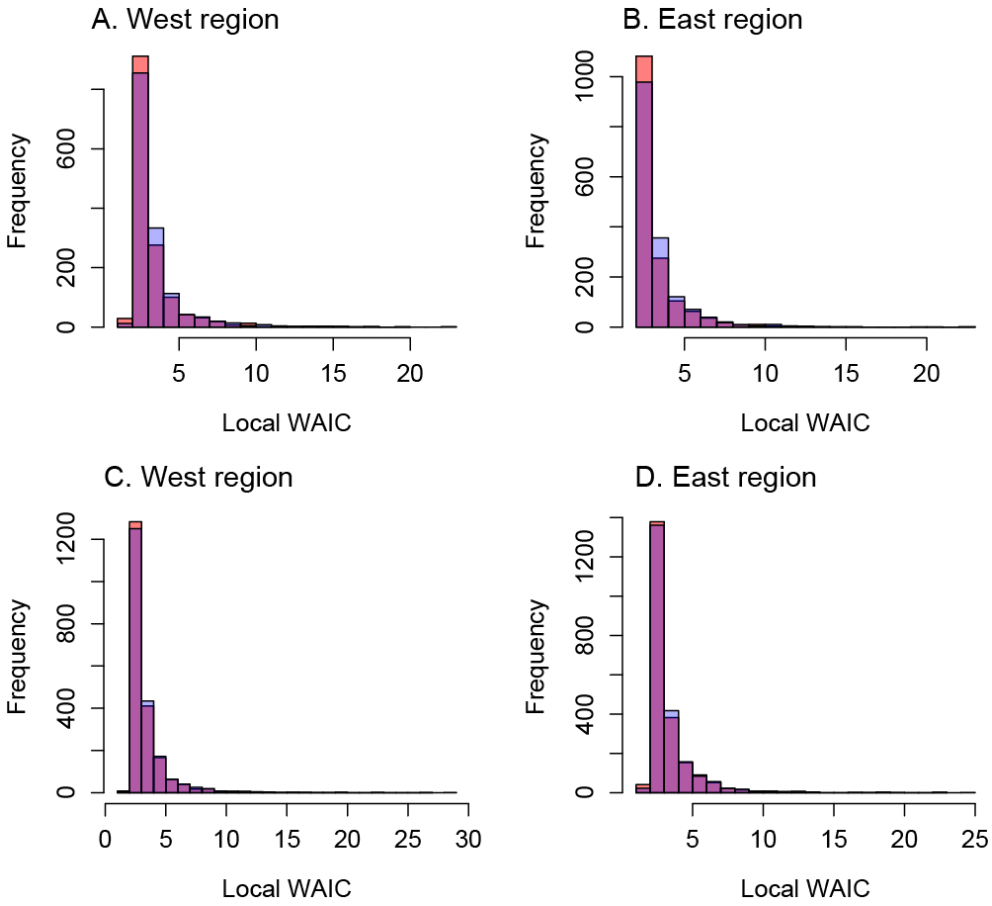

Figure S10. The distribution of the WAIC values for each data point. **A-B**. Results for the LMC (red) and a geostatistical model that excludes resistance interactions across insecticides (blue) fitted to bioassay results for the three pyrethroid types are shown. **C-D.** Results for the LMC (red) and a geostatistical model that excludes resistance interactions between DDT and pyrethroids (blue) fitted to bioassay results for DDT and the three pyrethroid types.

S2.4. Other posterior predictive checks

We also compared the distribution of the proportional mortality observations for each insecticide type across all sample collection locations and times with the posterior distribution of the model predictions at these same locations and times. Posterior distributions of the predicted values were based on 10000 draws from the posterior (obtained using the "inla.posterior.sample()" function; http://www.r-inla.org). The distributions of observed and simulated data are similar for the west region (Fig. S11) and for the east region (Fig. S12).

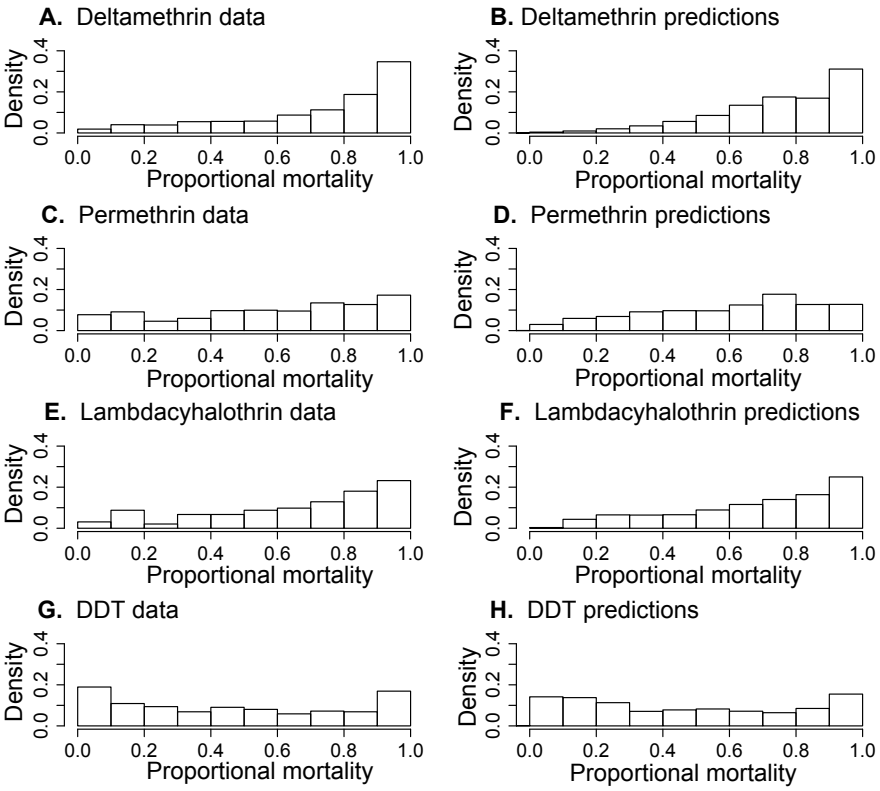

Figure S11. Comparing histograms of the bioassay observations for the west region with histograms of posterior simulations of these data.

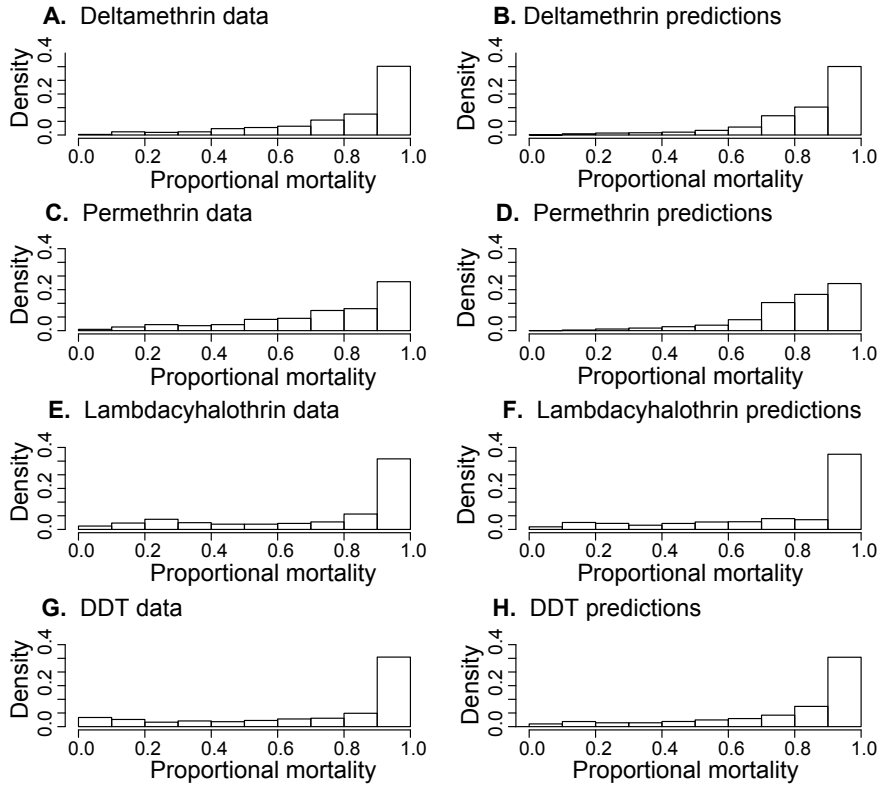

Figure S12. Comparing histograms of the bioassay observations for the east region with histograms of posterior simulations of these data

S3. Predicted cross-insecticide interaction strengths for models incorporating pyrethroids and DDT

We compared the posterior distributions of the coefficients of $\lambda_{(\bullet,\bullet)}$ of the predicted interactions between the predicted prevalence of resistance across different insecticide types (see eqn 2 and section S6) produced by the LMC fitted to the west and east regions. For the LMC fitted to the bioassay data for three pyrethroid types, the posterior distributions for both regions overlap in the case of all coefficients (Fig. S13). This indicates that the strength of the predicted interactions between the three pyrethroid types is similar across the two regions. We also assessed whether resistance relationships across the pyrethroid insecticides could be parsimoniously assessed by fitting a single LMC to the full set of bioassay data combined across the two separate regions. We note that this approach requires the assumption of stationarity to be applied across a much larger spatial area (see section S6). This single model showed lower predictive accuracy compared to the two separate LMCs for each region. The single model produced a WAIC of 10089.68 which is substantially higher than the sum of the WAIC values over the two separate models (9824.22). The single model also produced an RMSE for the 10-fold out-of-sample validation of 0.180, which is higher than the RMSE of 0.175 produced by 10-fold out-of-sample validation across the combined withheld data for the two separate models. We therefore conclude that applying separate model fits to each separate spatial region, and avoiding the assumption of stationarity across a larger spatial scale, is preferable.

For the LMC fitted to the bioassay data for the DDT and the three pyrethroid types, there is a credible difference between the posterior distributions of $\lambda_{A,D}$ (the coefficient describing the strength of the interaction between predicted resistance to deltamethrin and DDT) for the west and east regions (Fig. S14A). This difference contributes to the differences in the form of the predicted resistance relationships between DDT and the three pyrethroid types seen in Fig. 3.

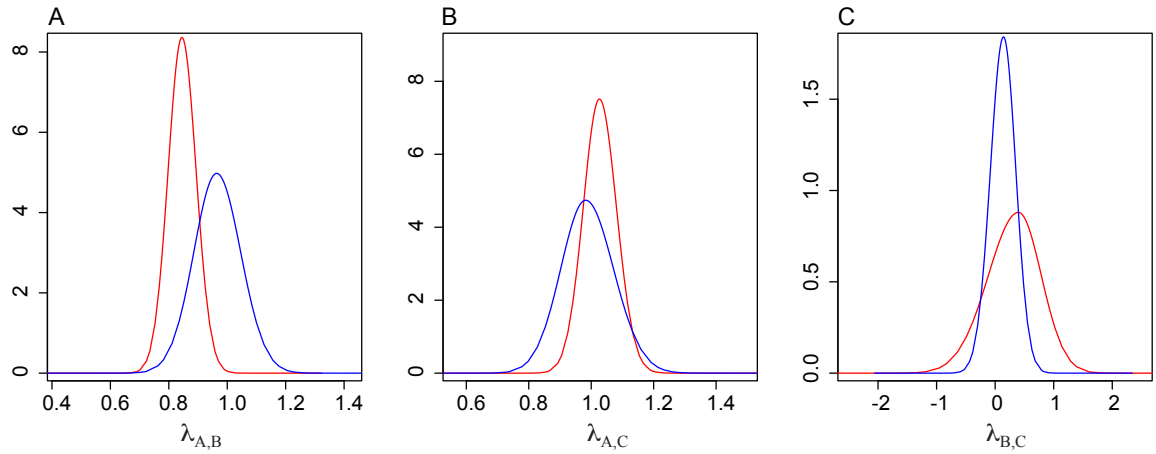

Figure S13. Posterior distributions of the coefficients of predicted interactions between **A.** Deltamethrin and permethrin. **B.** Deltamethrin and lambdacyhalothrin. **C.** Permethrin and λ-cyhalothrin. Blue and red lines show

the models fitted to the pyrethroid bioassay data from the west and east regions, respectively.

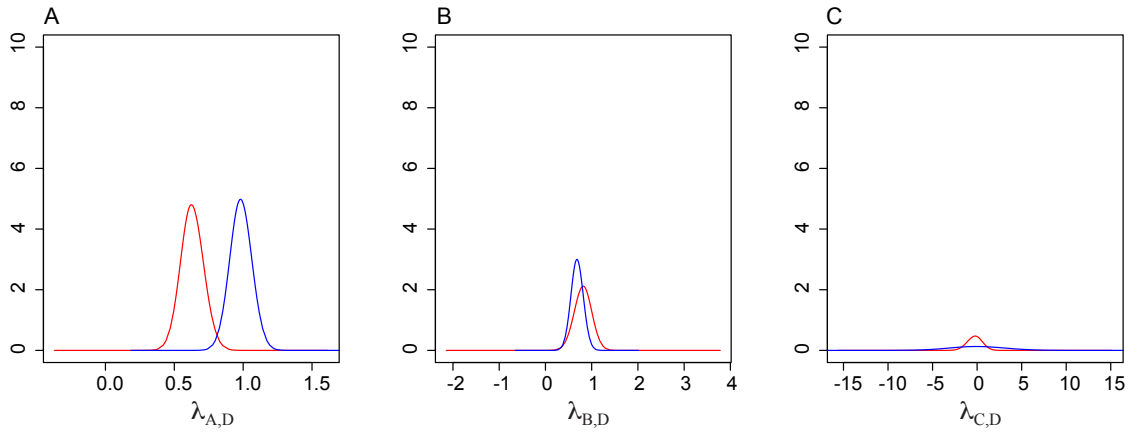

Figure S14. Posterior distributions of the coefficients of predicted interactions between **A.** Deltamethrin and DDT. **B.** Permethrin and DDT. **C.** λ-cyhalothrin and DDT. Blue and red lines show the models fitted to the pyrethroid bioassay data from the west and east regions, respectively.

S4. Predicted resistance relationships across the other insecticide combinations

For models which included bioassay results for all other combinations of insecticide classes, the LMC which included interactions between resistance across insecticide classes did not perform better than a model which assumed independence of resistance across insecticide classes. The lack of interaction predicted by the LMC is visually apparent and two examples are given (Figs. S15 & S16).

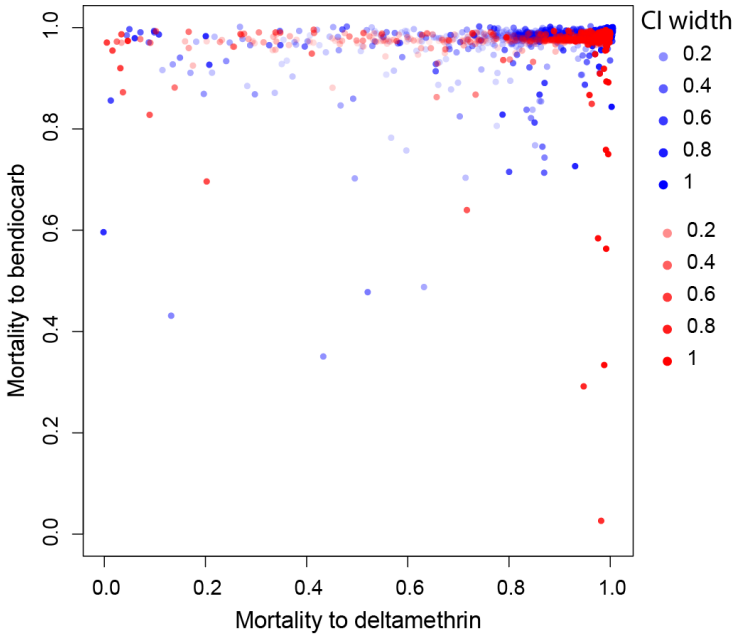

Figure S15. Predicted mean proportional bioassay mortality to bendiocarb vs deltamethrin. Points show the predicted mean at each location and time for the

west region (blue) and the east region (red). Colour intensity indicates the width of the posterior credible interval (CI) of the predicted mean.

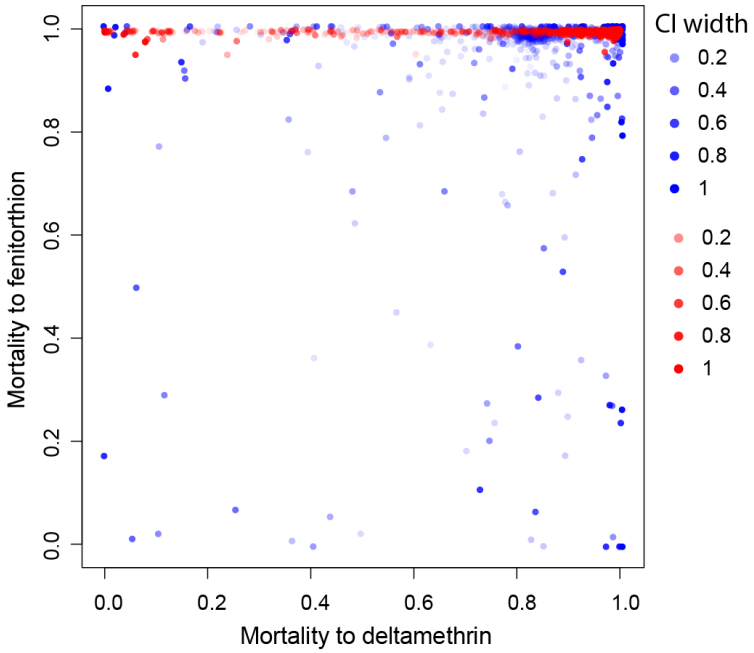

Figure S16. Predicted mean proportional bioassay mortality to fenitrothion vs deltamethrin. Points show the predicted mean at each location and time for the west region (blue) and the east region (red). Colour intensity indicates the width of the posterior credible interval (CI) of the predicted mean.

S5. Analysis of linear associations between DDT and pyrethroid resistance and the prevalence of *Vgsc* point mutations

We used ordinary least squares (OLS) linear regression models to assess associations between predicted mean resistance to DDT and the three pyrethroids and the observed frequency of *Vgsc* mutations in field-collected *Anopheles gambiae* complex samples. We included two covariates, the frequency of L1014L and L1014S mutations, noting that these covariates also account for the frequency of the only other allele type, L1014F. Using cluster robust standard errors (15, 16), we found significant associations between predicted mean mortality following exposure to DDT and the prevalence of the L1014L and L1014S *Vgsc* alleles (Table S3). In the case of predicted mean mortality following exposure to deltamethrin, permethrin or λ-cyhalothrin, we found a significant effect of either type of *Vgsc* mutation but there was no significant effect of the particular type of mutation (L1014F or L1014S) (Table S3).

Insecticide type	**Intercept (SE)**	**L1014L (SE)**	**L1014S (SE)**
DDT	1.48 (0.24)*	0.61 (0.05)*	0.31 (0.06)*
Deltamethrin	2.38 (0.3)*	0.27 (0.06)*	-0.01 (0.07)
Permethrin	1.37 (0.24)*	0.31 (0.05)*	0.08 (0.06)
λ-cyhalothrin	1.46 (0.33)*	0.27 (0.06)*	0.04 (0.08)

Table S3. Results of linear regression model fits using predicted mean mortality to DDT and three different pyrethroid types as the response variable and the

observed prevalence of each type of *Vgsc* mutation as the two dependent variables. Asteriks (*) denote $P < 0.05$.

S6. Spatio-temporal Bayesian statistical models

We start by defining a Bayesian hierarchical formulation of our model of the proportional mortality records for bioassays conducted using a single insecticide type *A* (eqn 1) as follows:

$$g_A(\mathbf{s}_i,t) \mid u_A(\mathbf{s}_i,t),\theta_A \sim N(\beta_A + \mathbf{A}u_A(\mathbf{s}_i,t),\sigma_A^2) \quad \text{(S1a)}$$

$$u_A(\mathbf{s}_i,t) = \phi_A u_A(\mathbf{s}_i,t-1) + \omega_A(\mathbf{s}_i,t) \quad \text{(S1b)}$$

where

$$Cov(\omega_A(\mathbf{s}_i,t),\omega_A(\mathbf{s}_j,t')) = \begin{Bmatrix} 0, & t \neq t' \\ \sigma^2_{\omega_A} C_A(h), & t = t' \end{Bmatrix} \quad \text{(S1c)}$$

and

$\theta_A \sim \boldsymbol{\pi}_A$

where $\boldsymbol{\pi}_A$ is a vector of prior probability distributions for the hyperparameters $\theta_A = [\beta_A, \sigma_A, \sigma_{\omega_A}, \kappa_A, \phi_A]$ (see section S6.1 for their specification) and $u_A(\mathbf{s}_i,t)$ is a spatio-temporal Gaussian Markov Random Field (GMRF; (17)). β_A and σ_A are a fixed intercept and the standard deviation of the observation noise, respectively (as defined in the Methods section of the main text), $\sigma_{\omega_A}, \kappa_A$ and ϕ_A are parameters of the GMRF (see below), and **A** is a sparse observation matrix that maps the GMRF to function evaluations at local observations. The spatio-temporal GMRF, $u_A(\mathbf{s}_i,t)$, is composed of a spatial GMRF that evolves according to a first order temporal auto-regressive process (AR(1)) with correlation ϕ_A (18). The innovation noise $\omega_A(\mathbf{s}_i,t)$ is a temporally uncorrelated Gaussian process with variance $\sigma^2_{\omega_A}$ and a spatial correlation structure $C_A(h)$ that is constant in time and defines the spatial dependence structure of the observations (19). Our spatial GMRF model follows the Integrated Nested Laplace Approximation (INLA) approach (Lindgren et al. 2011), whereby we assume that $C_A(h)$ is a Matérn covariance function. In developing the INLA approach, Lindgren et al. (2011) used the Matérn covariance function to define an approximation to a GMRF using stochastic partial differential equations. The Matérn covariance function $C_A(h)$ depends on the spatial separation distance between two points, $h = \left\| \mathbf{s}_i - \mathbf{s}_j \right\|$ as well as a scale parameter κ_A and a fixed smoothness parameter ν which is set to 1. The spatial process is therefore assumed to be second-order stationary and isotropic (19).

To jointly model bioassay mortality observations for two insecticides *A* and *B* we combine eqns (S1) with an additional hierarchical model that introduces a link between mortality for the two insecticides through the spatial component of the mean, $u_A(\mathbf{s}_i,t)$:

$$g_B(\mathbf{s}_i,t) \mid u_B(\mathbf{s}_i,t), u_A(\mathbf{s}_i,t), \theta_B, \sigma_{\omega_A}, \kappa_A, \phi_A \sim N(\beta_B + \lambda_{B,A}\mathbf{A}u_A(\mathbf{s}_i,t) + \mathbf{A}u_B(\mathbf{s}_i,t), \sigma_B^2) \quad \text{(S2a)}$$

$$u_B(\mathbf{s}_i,t) = \phi_B u_B(\mathbf{s}_i,t-1) + \omega_B(\mathbf{s}_i,t) \quad \text{(S2b)}$$

where

$$Cov(\omega_B(\mathbf{s}_i,t),\omega_B(\mathbf{s}_j,t')) = \begin{cases} 0, & t \neq t' \\ \sigma^2_{\omega_B} C_B(h), & t = t' \end{cases} \quad \text{(S2c)}$$

and

$\theta_B \sim \boldsymbol{\pi}_B$

where $\boldsymbol{\pi}_B$ is a vector of prior probability distributions for the hyperparameters $\theta_B = [\beta_B, \lambda_{B,A}, \sigma_B, \sigma_{\omega_B}, \kappa_B, \phi_B]$ (section S6.1). The spatio-temporal GMRF, $u_B(\mathbf{s}_i,t)$, has variance $\sigma^2_{\omega_B}$ and a Matérn covariance function, $C_B(h)$ with scale and smoothness parameters κ_B and ν. The coefficient $\lambda_{B,A}$ describes the strength of the interaction between predicted prevalence of resistance to the two insecticides. We implement the models (S1) and the joint model given by (S1) and (S2) using the R-INLA package (http://www.r-inla.org) to obtain estimates of the posterior distributions of $u_A(\mathbf{s}_i,t)$, $u_B(\mathbf{s}_i,t)$, θ_A and θ_B.

Our LMC models of bioassay mortality observations for up to four insecticide types, *A*, *B*, *C* and *D,* were developed using a straightforward extension of the approach specified in the main text (eqns (1) and (2)) using the above Bayesian hierarchical method (eqns (S1) and (S2)). Thus, our models of the logit transformed mortality observations for insecticides *C* and *D* are given by:

$$g_C(\mathbf{s}_i,t) = \beta_C + \lambda_{C,A} u_A(\mathbf{s}_i,t) + \lambda_{C,B} u_B(\mathbf{s}_i,t) + u_C(\mathbf{s}_i,t) + e_C \quad \text{(S3)}$$

$$g_D(\mathbf{s}_i,t) = \beta_D + \lambda_{D,A} u_A(\mathbf{s}_i,t) + \lambda_{D,B} u_B(\mathbf{s}_i,t) + \lambda_{D,C} u_C(\mathbf{s}_i,t) + u_D(\mathbf{s}_i,t) + e_D \quad \text{(S4)}$$

where $u_C(\mathbf{s}_i,t)$ and $u_D(\mathbf{s}_i,t)$ are GMRFs defined in the same way as $u_B(\mathbf{s}_i,t)$ and $u_A(\mathbf{s}_i,t)$ (eqns (S1b,c) and (S2b,c)) and $\lambda_{C,A}$, $\lambda_{C,B}$, $\lambda_{D,A}$, $\lambda_{D,B}$ and $\lambda_{D,C}$ are constant coefficients. We define the probability of $g_C(\mathbf{s}_i,t)$ conditional on β_C, $\lambda_{C,A}$, $\lambda_{C,B}$, σ_C, as well as $u_C(\mathbf{s}_i,t)$, $u_B(\mathbf{s}_i,t)$, $u_A(\mathbf{s}_i,t)$ and their variance, scale and smoothness parameters, similarly to eqn (S2a). The conditional probability for $g_D(\mathbf{s}_i,t)$ is defined by continuing this hierarchical procedure.

For the organophosphates class we have a small number of observations for two insecticide types, fenitrothion and malathion, which we denote A_1 and A_2. To model resistance to these two insecticides we modify eqn (S1a) to allow resistance to each insecticide to differ by a fixed effect:

$$\begin{aligned} g_{A_1}(\mathbf{s}_i,t) \mid u_A(\mathbf{s}_i,t), \theta_A &\sim N(\beta_{A_1} + \mathbf{A} u_A(\mathbf{s}_i,t), \sigma^2_A) \\ g_{A_2}(\mathbf{s}_i,t) \mid u_A(\mathbf{s}_i,t), \theta_A &\sim N(\beta_{A_2} + \mathbf{A} u_A(\mathbf{s}_i,t), \sigma^2_A) \end{aligned} \quad \text{(S5)}$$

The two constants β_{A_1} and β_{A_2} are then included into the vector of hyperparameters, θ_A.

S6.1. Prior distribution specification

For the model with a single response variable (eqns S1) we use a PC precision prior (Krainski 2017; Simpson et al. 2017) for the standard deviations σ_A and σ_{ω_A} setting the upper limit U = 5 and the probability α=0.01. Our prior for κ_A is given by setting a PC prior on the range parameter (20) setting the lower limit U=0.0003 and the probability α=0.01, noting that we define spatial locations

using a 3D Cartesian coordinate system. Our prior for ϕ_A is a PC prior for the correlation parameter in a first order autoregressive (AR(1)) model (20) where we set the upper limit U=0.5 and the probability α =0.5. For β_A we use a Gaussian distribution with a mean of zero and a precision parameter τ =0.001. For our joint models of multiple response variables (eqns S2-S4) we use these same standard deviation, range, AR(1) correlation parameter and fixed effect prior distributions. We use Gaussian priors with a mean of zero and a precision parameter τ =0.1 for each of the random effect coefficients $\lambda_{(\bullet,\bullet)}$.

S7. *Vgsc* allele frequency data selection criteria

If allele frequencies were provided for subsamples that split out either individual species or dead/alive mosquitoes, these values were only combined and used if no selection was performed that could bias the proportion of species or dead/alive mosquitoes and thus potentially bias the allele frequency for the species complex sample. For example, results that only provided allele frequencies for one species from a multi-species sample were excluded. Likewise, results for subsamples selected to include equal numbers of dead and alive mosquitoes were also excluded. This protocol accounted for cases where, according to the information reported, the original sample was manipulated by drawing one or more subsets, subdivision, or both subsetting and subdivision. We only included results for three types of samples: 1. Samples that had not been subsetted or subdivided. 2. Samples which had been subdivided but not subsetted. 3. Samples that had been randomly subsampled and not subdivided. In cases where the sample had been subdivided we also required that the number of mosquitoes in each subset be reported. We then calculated the *Vgsc* allele prevalence in the total sample combined across the subsets. In addition, we also excluded records where the *Vgsc* allele prevalence was based on a total sample size of less than 40 mosquitoes or where the sample collection location could not be assigned a point coordinate.

References

1. Coleman M, Hemingway J, Gleave KA, Wiebe A, Gething PW, Moyes CL. Developing global maps of insecticide resistance risk to improve vector control. Malaria Journal. 2017;16.
2. Antonio-Nkondjio C, Sonhafouo-Chiana N, Ngadjeu CS, Doumbe-Belisse P, Talipouo A, Djamouko-Djonkam L, et al. Review of the evolution of insecticide resistance in main malaria vectors in Cameroon from 1990 to 2017. Parasites & Vectors. 2017;10.
3. Awolola TS, Oduola OA, Strode C, Koekemoer LL, Brooke B, Ranson H. Evidence of multiple pyrethroid resistance mechanisms in the malaria vector Anopheles gambiae sensu stricto from Nigeria. Transactions of the Royal Society of Tropical Medicine and Hygiene. 2009;103(11):1139-45.
4. Brooke BD, Kloke G, Hunt RH, Koekemoer LL, Temu EA, Taylor ME, et al. Bioassay and biochemical analyses of insecticide resistance in southern African Anopheles funestus (Diptera : Culicidae). Bulletin of Entomological Research. 2001;91(4):265-72.

5. Nardini L, Christian RN, Coetzer N, Ranson H, Coetzee M, Koekemoer LL. Detoxification enzymes associated with insecticide resistance in laboratory strains of *Anopheles arabiensis* of different geographic origin. Parasites & Vectors. 2012;5.
6. Nardini L, Hunt RH, Dahan-Moss YL, Christie N, Christian RN, Coetzee M, et al. Malaria vectors in the Democratic Republic of the Congo: the mechanisms that confer insecticide resistance in Anopheles gambiae and Anopheles funestus. Malaria Journal. 2017;16.
7. Pinto J, Lynd A, Vicente JL, Santolamazza F, Randle NP, Gentile G, et al. Multiple Origins of Knockdown Resistance Mutations in the Afrotropical Mosquito Vector Anopheles gambiae. Plos One. 2007;2(11).
8. Riveron JM, Irving H, Ndula M, Barnes KG, Ibrahim SS, Paine MJI, et al. Directionally selected cytochrome P450 alleles are driving the spread of pyrethroid resistance in the major malaria vector *Anopheles funestus*. Proceedings of the National Academy of Sciences of the United States of America. 2013;110(1):252-7.
9. Sangba MLO, Sidick A, Govoetchan R, Dide-Agossou C, Osse RA, Akogbeto M, et al. Evidence of multiple insecticide resistance mechanisms in *Anopheles gambiae* populations in Bangui, Central African Republic. Parasites & Vectors. 2017;10.
10. Santolamazza F, Calzetta M, Etang J, Barrese E, Dia I, Caccone A, et al. Distribution of knock-down resistance mutations in Anopheles gambiae molecular forms in west and west-central Africa. Malaria Journal. 2008;7.
11. Yahouedo GA, Chandre F, Rossignol M, Ginibre C, Balabanidou V, Mendez NGA, et al. Contributions of cuticle permeability and enzyme detoxification to pyrethroid resistance in the major malaria vector *Anopheles gambiae*. Scientific Reports. 2017;7.
12. World Health Organization. Test procedures for insecticide resistance monitoring in malaria vector mosquitoes. Geneva: WHO, 2016.
13. Czado C, Gneiting T, Held L. Predictive Model Assessment for Count Data. Biometrics. 2009;65(4):1254-61.
14. Held L, Schrodle B, Rue H. Posterior and Cross-validatory Predictive Checks: A Comparison of MCMC and INLA. Kneib T, Tutz G, editors2010. 91-110 p.
15. Cameron AC, Miller DL. A Practitioner's Guide to Cluster-Robust Inference. Journal of Human Resources. 2015;50(2):317-72.
16. Conley TG. GMM estimation with cross sectional dependence. Journal of Econometrics. 1999;92(1):1-45.
17. Rue H, Held L. Gaussian Markov Random Fields: Theory and Applications: Chapman and Hall; 2005. 280 p.
18. Bhatt S, Weiss DJ, Cameron E, Bisanzio D, Mappin B, Dalrymple U, et al. The effect of malaria control on *Plasmodium falciparum* in Africa between 2000 and 2015. Nature. 2015;526(7572):207-2011.
19. Cameletti M, Lindgren F, Simpson D, Rue H. Spatio-temporal modeling of particulate matter concentration through the SPDE approach. Asta-Advances in Statistical Analysis. 2013;97(2):109-31.
20. Fuglstad G, Simpson D, Lindgren F, Rue H. Constructing priors that penalize the complexity of gaussian random fields. submitted. 2017.